ISSN 2616-5767 Vol.5, Issue 6: 49-54, DOI: 10.25236/AJETS.2022.050609

Numerical simulation of multi-physical field coupling of a piezoelectric pump with flexible valve at an optimal working point

Lu Wang, Jinlan Yang, Linjiao Li, Jun Huang*

Research Center of Fluid Machinery Engineering and Technology, Jiangsu University, Zhenjiang, 212013, China

Abstract: *A piezoelectric pump with flexible valve was proposed for living cells transmission to avoid the cell damage caused by valve material during transmitting process. However, the dynamic switching characteristics of the flexible valve coupled with the flow field directly affected both the flow field inside the pump chamber and the output performance of the pump. At the same time, the output performance of the piezoelectric pump mainly took the optimal working point as a standard. Therefore, the electric-solid-liquid multi-physical field coupling finite element model of the piezoelectric pump with flexible valve based on dynamic mesh was established to study the dynamic characteristics of the valve and the transient flow characteristics of the flow field under the optimal working point. The calculation results of the flow rate show that the output flow rate of the pump is 6.19 g/min at the optimal working point (200 V_{PP}, 10 Hz). The error is 8.94 % compared with the experimental flow rate, which verifies the accuracy of the calculation model. The results of this paper can provide a reference for multi-physical field coupling calculation and optimization design of valve-based piezoelectric pumps with different structures.*

Keywords: *flexible valve; piezoelectric pump; multi-physical field coupling*

1. Introduction

In recent years, with the rapid development of tissue engineering and micro-nano processing technology, organ chips based on microfluidic chip technology are becoming a new field in bio-medicine[1–3]. Micro-pumps are usually connected with organ chips to construct a dynamic in vitro model of circulation to veritably simulate the physiological environment in vivo. Micro-pumps are required to have simple structure, easy to integrate and no damage to cells[4]. Therefore, different types of micro-pumps are developed and used to drive cell culture medium on organ chips. Piezoelectric micro-pump has been widely studied and applied in bio-medicine and other fields due to its simple structure, rapid response, high energy density and no electromagnetic interference[5-7].

Based on the application requirements in different fields, researchers have designed various types of piezoelectric pumps. The piezoelectric pump is divided into valveless piezoelectric pump and valve-based piezoelectric pump[8,9] according to whether there is a valve inside the pump chamber. Valveless piezoelectric pump has simple structure, small volume, and good reliability because of no moving parts. However, since there is no valve movement, the output performance of such pumps have periodic pulsation and the output flow rate is uncontrollable. Valve-based piezoelectric pump has a better output performance and controllability than valveless piezoelectric pump. However, the working frequency of valve-based piezoelectric pump is high, which is easy to cause large shear stress of the fluid, and the valves are mostly made of hard materials, which is not suitable for the transmission of living cells, thus its application in bio-medicine and other fields is limited. To solve this problem, inspired by the structure of human heart aortic valve, a piezoelectric pump with flexible valve was designed[10]. The flow rate test showed that the pump could effectively realizes the fluid transmission.

As a valve-based piezoelectric pump, the dynamic characteristics of the flexible valve have a crucial impact on the flow field in the pump chamber and the output performance of the pump. Meanwhile, the output performance of micro-pump mainly takes the optimal working point as a standard. Therefore, based on the structure design of the piezoelectric pump with flexible valve in our previous work, this study established the electric-solid-liquid multi-physical field coupling finite element model of the piezoelectric pump with flexible valve, then analyzed the switching characteristics of the flexible valve

ISSN 2616-5767 Vol.5, Issue 6: 49-54, DOI: 10.25236/AJETS.2022.050609

and the flow characteristics of the flow field in the pump chamber under the optimal working point. The research results provide a theoretical support for the structural optimization of the piezoelectric pump with flexible valve.

2. Design of the piezoelectric pump with flexible valve

Prototype processing and testing were carried out according to the piezoelectric pump with flexible valve designed in the previous research[10]. The whole piezoelectric pump with flexible valve is composed of a flexible valve (divided the pump chamber into an upper pump chamber and a lower pump chamber), a pump body containing a contraction/diffusion tube, a piezoelectric vibrator and inlet/outlet flow tube. The lobe facing the outlet diffuser is defined as the lobe A, and the other two lobes are named as lobe B and lobe C respectively in a clockwise direction. The ridges of lobe B and lobe C are parallel to the inlet and outlet conical flow channels. The external dimensions of the pump body are 106 mm×56 mm×18 mm, the internal structure parameters and annotations are shown in Fig. 1. A prototype of piezoelectric pump with flexible valve was processed, the material of flexible valve is Stratasys tango agilus 30 rubber material (Shore's hardness is 30 HA) and the material of the pump body is light-sensitive resin.

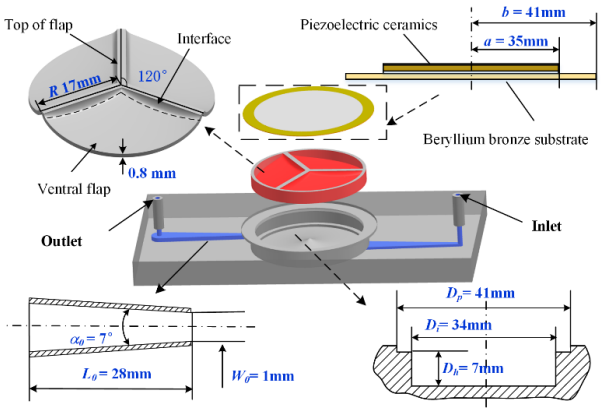

Figure 1: Structure diagram of the piezoelectric pump with flexible valve

The experimental setup and procedure of the piezoelectric pump with flexible valve have been described in Ref. 10. When the driving frequency is 10 Hz, the output flow rate of the pump reaches the maximum value of 5.68 g/min, which is defined as the optimal working point.

3. Establishment of multi-physical field coupling model

The three-dimensional model of the piezoelectric pump with flexible valve was established. The free tetrahedral mesh was used to mesh the piezoelectric vibrator, valve body and water body calculation domain, and the meshes at throat and bias area were locally encrypted.

When analyzing the structural model of the piezoelectric pump with flexible valve, it is necessary to take the coupling effect between piezoelectric actuator and fluid in the pump chamber into account, as well as the coupling relationship between flexible valve and fluid. The calculation modules adopted include: the interaction between fluid and solid (fluid-solid coupling) and the interaction between solid piezoelectric plate and electrostatic field (piezoelectric effect).

In this research, because the internal flow of the piezoelectric pump with flexible valve is a pulsating flow with low Reynolds number, which leads to the continuous state change of the flexible valve, so the Realizable $k-\varepsilon$ turbulence model in published literature[11] can be used to simulate and solve the problem in this study.

The piezoelectric material is PZT-5A with the diameter of 35mm and thickness of 0.21mm. The driving voltage applied on the upper surface is $V_0 \cdot \sin(\omega t)$, and the outer boundary is set as a fixed constraint. The super-elastic compressible material was used for fabricating the flexible valve, and the material model was Neo-Hookean. The edge of the flexible valve was set as a fixed constraint.

The boundary conditions of the fluid domain were set as follows, it was assumed that: (1) the fluid medium was incompressible; (2) the physical property parameters of the fluid remained the same with the change of temperature; (3) the influence of gravity on fluid was neglected; (4) there was no slippage

ISSN 2616-5767 Vol.5, Issue 6: 49-54, DOI: 10.25236/AJETS.2022.050609

between the fluid and the wall. The inlet and outlet were set as pressure boundary conditions, the pressure was 0 Pa, the fluid medium was water, the density was 1000kg/m^3 and the dynamic viscosity was 1×10^{-3}Pa·s.

The computational domain boundaries of solid contact with fluid were all set as FSI boundaries. The solver type was fully coupled and the solution method is iterative solution.

4. Results and discussion

Fig. 2 shows the displacement response curve of the free end of the flexible valve with multi-physical field coupling in Z direction. Fig. 3 shows the displacement nephogram of the flexible valve at 0T, T/4, T/2 and 3T/4 respectively. It can be seen from Fig. 4 that the time from 0T to T is a complete vibration period of the piezoelectric pump with flexible valve; from 0T to T/4 and from 3T/4 to T are suction mode of the piezoelectric pump with flexible valve, and from T/2 to 3T/4 is pumping mode of the piezoelectric pump with flexible valve. From Fig. 2 and Fig. 3, we can see that the displacements of three lobes were different at the same time, while the maximum displacement of lobe A was greater than the maximum displacements of lobes B and C. In addition, the displacement curves of lobes B and C were coincided, and the switch displacement of lobe A lagged lobes B and C. At 0 T, the pump was in the middle stage of suction mode. Some fluid entered in the pump chamber from the outlet contraction/diffusion channel, and then impacting the lobe A that was opening (rising), resulting in the opening speed of lobe A lagging behind the opening speed of lobes B and C. At T/4, the displacements of the three lobes were basically the same, but the lobe A was in the opening (ascending) stage, and the opening lag effect appeared, while the lobes B and C were in the closing (descending) stage, showing an advanced closing effect. The maximum displacement of the lobe was 70μm. At T/2, lobes B and C had fallen to the lowest point, with the maximum reverse displacement of 80μm, while lobe A was in rapid closure stage. At this moment, the pump was in the middle of the pumping mode. The fluid above the lobe discharged the pump chamber through the outlet flow channel, and the fluid below the lobe was compressed by three lobes and outflows from the inlet channel. At 3T/4, the piezoelectric pump was at the transition point between pumping mode and suction mode. At this moment, the lobe A had the maximum reverse displacement of 80μm, while the lobes B and C had already in the opening stage. Fig. 2 and Fig. 3 reflectes the influence of the inlet and outlet channels of the piezoelectric pump when the flexible valve is integrated into the piezoelectric pump. Each lobe shows different response posture and working characteristics.

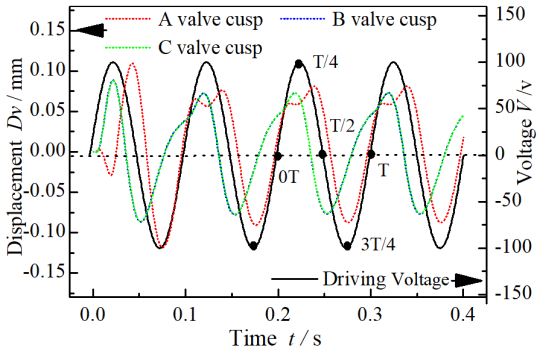

Figure 2: Free end displacement curve of the flexible three-lobe

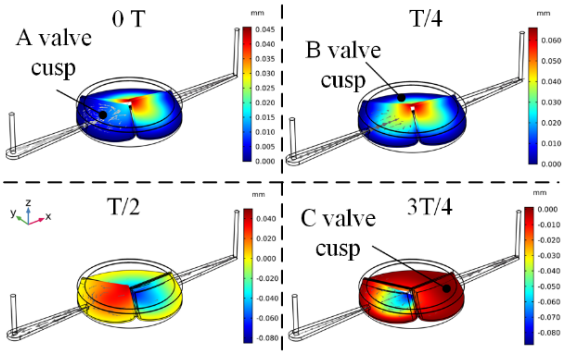

Figure 3: Displacement distribution of the flexible valve at different moments

ISSN 2616-5767 Vol.5, Issue 6: 49-54, DOI: 10.25236/AJETS.2022.050609

The two-dimensional flow field distribution inside the pump chamber was observed by selecting the middle section 1 of the inlet channel and the middle section 2 of the outlet channel. Fig. 4 shows the velocity streamline distribution of section 1 and section 2. At 0T (t=0.2s), the piezoelectric pump was in the middle stage of inhalation, and the fluid entered from the inlet diffuser and the outlet contraction tube respectively. After the fluid entered in the pump chamber from the inlet diffuser, the mainstream diffused and then gathered on the other side, where the velocity was approximately 0 m/s; while the fluid entered the pump chamber from the outlet contraction tube, the main flow diffused after extrusion by small-scale symmetrical vortices, and was affected by the large-scale symmetrical vortices. The cross section of the main channel becomes narrowed, then the velocity increased significantly. After being affected by the free end walls of three-lobe, the fluid gradually evolved into the new vortices. At T/4 (t=0.225s), the piezoelectric pump shifted from suction mode to pumping mode, and there was still fluid flowing from both channels of the pump chamber due to the inertial force, but the speed was very slow. Symmetrical vortex regions appeared at the connection area of section 1 inlet and the pump chamber, where one part of the mainstream would diffuse, and the other part would deviate due to the influence of the wall surface of pump chamber, then they would gather on both sides of pump chamber. When the fluid entered the pump chamber through the contraction tube, the mainstream was affected by the large-scale re-circulation zones on both sides, and the velocity increased significantly when it passed through the vortex core areas. The main reason was that after the mainstream was squeezed by the large-scale vortices, then cross-sectional of the channel further narrowed, therefore the velocity increased. At T/2 (t=0.25s), the piezoelectric pump was in the middle of the pumping mode. At this moment, the structure of the instantaneous flow field in section 1 and section 2 had changed significantly, and the diffusion tube in suction mode became the contraction tube in pumping mode. The fluid element in section 1 started from a point at right, then it was squeezed by the wall surface of the pump chamber after diffusion. The vortex areas were formed by the interaction with the mainstream and the outlet, which hindered the flow. The large-scale vortex regions of section 2 gradually evolved into the mainstream regions along the diffusion channel, and then the fluid was discharged from the pump chamber. At 3T/4 (t=0.275s), the piezoelectric pump turned into suction mode, the fluid velocity in the pump chamber was very slow, and a small amount of fluid was still in pumping mode. There were many small-scale vortices and secondary flow regions in the pump chamber and the contraction tube of section 1, and the symmetric vortices that hindered the fluid flow to the contraction tube were not dissipated. The streamline distribution of section 2 was similar to that at T/2. After the vortex regions were extruded by the wall surface of the pump chamber, part of the vortex regions form the mainstream flowed into the diffusion tube, and the other part interacts with the vortex region then formed the backflow vortex again. The flow field near the lobes B and C was basically symmetrical. Due to the uneven distribution of fluid in the pump chamber, there were many secondary flow areas.

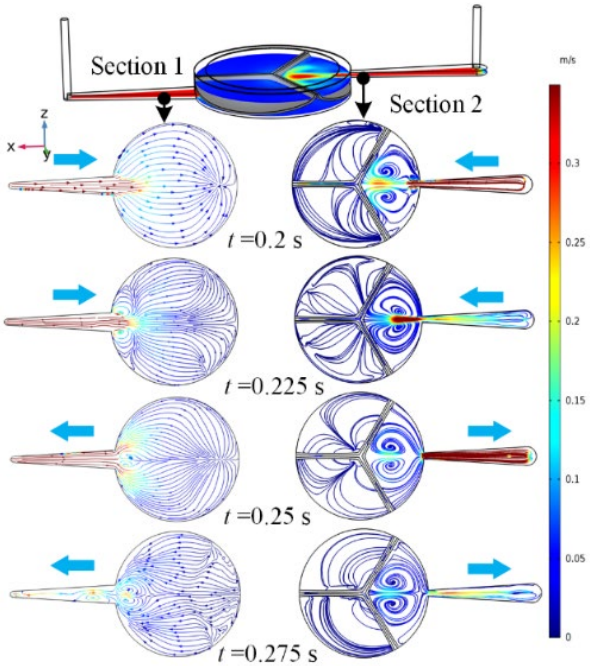

Figure 4: Flow line distribution on section 1 and section 2

ISSN 2616-5767 Vol.5, Issue 6: 49-54, DOI: 10.25236/AJETS.2022.050609

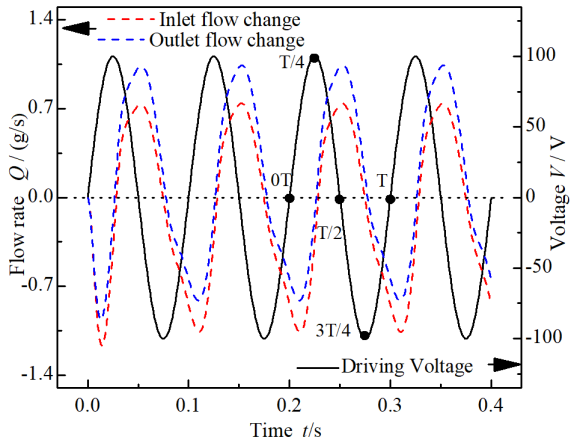

Figure 5: Inlet/outlet flow rate curves of the piezoelectric pump with flexible valve

The transient flow characteristics of the flow field in the piezoelectric pump with flexible valve have a significant influence on the opening and closing states of the valve as well as output performance. When the driving voltage is 200 V_{PP} and the driving frequency is 10 Hz, the inlet and outlet flow rate changes of the piezoelectric pump with flexible valve are shown in Fig. 5. A flow calculation curve in one period was selected and time integration was carried out to obtain the outlet flow rate simulation results of the piezoelectric pump with flexible valve at the optimal working point (200 V_{PP}, 10 Hz), the flow rate obtained was 6.19 g/min. The test showed that the output flow rate of the piezoelectric pump with flexible valve was 5.68 g/min at the optimal working point. The error between the simulation flow rate results and the test results was 8.94 % which verified the validity of the multi-physical field coupling calculation model.

5. Conclusions

The electro-solid-liquid multi-physical field coupling finite element model of the piezoelectric pump with flexible valve was established. The dynamic characteristics of the flexible valve body and the transient characteristics of the internal flow field in the pump chamber were analyzed under the optimal working point. Finally, the simulation results and experimental results were compared. The main findings of the study were summarized as follows:

(1) The opening and closing states of flexible valves are significantly affected by the inlet and outlet contraction/diffusion channels, and the opening and closing states of lobe A is different from that of lobes B and C at the same time. When the flexible valve interacts with the fluid medium, the stress is far less than the ultimate stress.

(2) The transient flow under the coupling of multiple physical fields is obviously affected by the opening and closing states of the flexible valve and the flow channel structure, and there are large-scale vortices and many secondary flow areas.

(3) The numerical calculation results show that the outlet flow rate of the piezoelectric pump is 6.19 g/min at the optimal working point, and the error compared with the experimental results is 8.94 % which verifies the validity of multi-physical field coupling calculation model.

References

[1] Zhang B, Korolj A, Lai B F L, et al. Advances in organ-on-a-chip engineering[J]. Nature Reviews Materials, 2018, 3(8): 257-278.
[2] Skardal A, Shupe T, Atala A. Organoid-on-a-chip and body-on-a-chip systems for drug screening and disease modeling[J]. Drug discovery today, 2016, 21(9): 1399-1411.
[3] Wagner I, Materne E M, Brincker S, et al. A dynamic multi-organ-chip for long-term cultivation and substance testing proven by 3D human liver and skin tissue co-culture[J]. Lab on a Chip, 2013, 13(18): 3538-3547.
[4] Li X, Liu S, Liang J, et al. Application of electroosmotic micropumps to a microfluidic system combined with a light-addressable potentiometric sensor[J]. physica status solidi (a), 2016, 213(6):

ISSN 2616-5767 Vol.5, Issue 6: 49-54, DOI: 10.25236/AJETS.2022.050609

1500-1504.
[5] Wang Y N, Fu L M. Micropumps and biomedical applications–A review[J]. Microelectronic Engineering, 2018, 195: 121-138.
[6] Hernandez C, Bernard Y, Razek A. A global assessment of piezoelectric actuated micro-pumps[J]. The European Physical Journal Applied Physics, 2010, 51(2): 20101.
[7] Yang Z, Zhou S, Zu J, et al. High-performance piezoelectric energy harvesters and their applications [J]. Joule, 2018, 2(4): 642-697.
[8] Hengyu Li, Junkao Liu, Kai Li, Yingxiang Liu, A review of recent studies on piezoelectric pumps and their applications, Mechanical Systems and Signal Processing, Volume 151,2021,107393.
[9] Maryam Hamlehdar, Alibakhsh Kasaeian, Mohammad Reza Safaei,Energy harvesting from fluid flow using piezoelectrics: A critical review, Renewable Energy, Volume 143,2019, Pages 1826-1838.
[10] Li Kai, Liu Jiaming, Zhang Quan, Zhang Jianhui, Huang Jun, Wang Yuan. A Flexible Valve Based Piezoelectric Pump for High Viscosity Cooling Liquid Transportation[J]. Transactions of Nanjing University of Aeronautics & Astronautics, 2021,38(6):993-1002.
[11] Guan Qingqiang. Study on Resistance Characteristics of Low Reynolds Number Pulsating Flow in Flexible Mini-channel[D]. Zhejiang University of Technology, 2020.